Quantum ratchets for periodically kicked cold atoms and Bose-Einstein condensates

2007 J. Phys.: Conf. Ser. 67 012001

(http://iopscience.iop.org/1742-6596/67/1/012001)

Journal of Physics: Conference Series **67** (2007) 012001 doi:10.1088/1742-6596/67/1/012001

Quantum ratchets for periodically kicked cold atoms and Bose-Einstein condensates

Giulio Casati[1,2] **and Dario Poletti**[1]

[1] Center for Nonlinear and Complex Systems, Università degli Studi dell'Insubria and Istituto Nazionale per la Fisica della Materia, Unità di Como, Via Valleggio 11, 22100 Como, Italy
[2] Department of Physics and Centre for Computational Science and Engineering, National University of Singapore, Singapore 117542, Republic of Singapore

E-mail: g0500502@nus.edu.sg

Abstract. We study cold atoms and Bose-Einstein condensates exposed to time-dependent standing waves of light. We first discuss a quantum chaotic dissipative ratchet using the method of quantum trajectories. This system is characterized by directed transport emerging from a quantum strange attractor. We then present a very simple model of directed transport with cold atoms in a pair of periodically flashed optical lattices.
Finally we study the dynamics of a dilute Bose-Einstein condensate confined in a toroidal trap and exposed to a pair of periodically flashed optical lattices. We show that the many-body atom-atom interactions, treated within the mean-field approximation, can generate directed transport.

1. Introduction

Cold atoms exposed to time-dependent standing waves of light provide an ideal testing ground to explore the features of the quantum dynamics of nonlinear systems. They allowed physicists to investigate experimentally several important physical phenomena, such as dynamical localization [1], decoherence [2], quantum resonances [3], and chaos assisted tunneling [4]. Very interestingly, they made it possible to realize experimentally the quantum kicked rotor [1, 2, 3], a paradigmatic model in the field of quantum chaos [5]. Lately, the use of cold atoms in optical lattices allowed to demonstrate the ratchet phenomenon [6], that is the presence of directed transport [7] in the absence of any net force. This phenomenon can be found in periodic systems due to a broken space-time symmetry [8], for example in presence of lattice asymmetry, unbiased periodic driving, and dissipation. Not only is the ratchet effect of potential relevance in technological applications such as rectifiers, pumps, particle separation devices, molecular switches and transistors, but it is also of great interest for the understanding of molecular motors in biology [9]. In this work we are going to present three different models of quantum ratchets. In Section 2 we present a model of a quantum ratchet in a dissipative chaotic system where the directed transport emerges from a quantum strange attractor. In Section 3 we study a different dissipative chaotic system which also presents a strange set. This model is very simple and therefore much easier to reproduce experimentally. In Section 4 we present an Hamiltonian ratchet where the directed transport emerges from the many-body interaction in a Bose-Einstein condensate (BEC). In Section 5 we present our conclusions.

2. Quantum ratchet in dissipative chaotic system

A characteristic feature of classical dissipative chaotic systems is the presence of strange attractors [10]. In quantum mechanics, it was found that the fractal structure of the classical strange attractor is smoothed on the scale of the Planck's cell [11]. It is therefore interesting to investigate how this phenomenon affects quantum ratchets [12].
In the following we consider a particle moving in one dimension [$x \in (-\infty, +\infty)$] in a periodic kicked asymmetric potential:

$$V(x,t) = k[\cos(x) + \frac{a}{2}\cos(2\,x + \phi)] \sum_{m=-\infty}^{+\infty} \delta(t - mT) \tag{1}$$

where T is the kicking period, k is the kicking strength, a is the relative strength of the second harmonic and ϕ ($\phi \in [0, 2\pi[$) is a parameter with breaks the space symmetry. It is very easy to see that the classical evolution of the system after one period is described by the map:

$$\begin{cases} \bar{n} = \gamma n + k(\sin(x) + a\sin(2x + \phi)) \\ \bar{x} = x + T\bar{n} \end{cases} \tag{2}$$

where n is the momentum variable conjugated to x and γ is the dissipation parameter, describing a velocity proportional damping ($0 \leq \gamma \leq 1$). Introducing the rescaled momentum variable $p = Tn$, it is seen that classical dynamics depends on the parameter $K = kT$ only. At $a = 0$ the classical model reduces to the Zaslavsky map [13].

By means of the usual quantization rules [5], $x \to \hat{x}$, $n \to \hat{n} = -i(d/d\hat{x})$ we obtain the quantum model. We set $\hbar = 1$ and since $[\hat{x}, \hat{p}] = iT$, the effective Planck constant is $\hbar_{eff} = T$. The classical limit corresponds to $\hbar_{eff} \to 0$, while keeping $K = \hbar_{eff} k$ constant.
To simulate a dissipative environment we consider a master equation in the Lindblad form [14] for the density operator $\hat{\rho}$ of the system:

$$\dot{\rho} = -i[\hat{H}_s, \hat{\rho}] - \frac{1}{2}\sum_{\mu=1}^{2}\{\hat{L}_\mu^+ \hat{L}_\mu, \hat{\rho}\} + \sum_{\mu=1}^{2} \hat{L}_\mu \hat{\rho} \hat{L}_\mu^+ \tag{3}$$

where $H_s = \hat{n}^2/2 + V(\hat{x}, t)$ is the system Hamiltonian, $\hat{L}_\mu$ are the Lindblad operators and $\{,\}$ denotes the anticommutator. We assume that the dissipation is described by the lowering o perators:

$$\begin{aligned} \hat{L}_1 &= \Gamma \textstyle\sum_n \sqrt{n+1}|n\rangle\langle n+1| \\ \hat{L}_2 &= \Gamma \textstyle\sum_n \sqrt{n+1}|-n\rangle\langle -n-1| \end{aligned} \tag{4}$$

with $n = 0, 1, ...$ These Lindblad operators can be obtained by considering the interaction between the system and a bosonic bath. The master equation Eq. (3) is then derived, at zero temperature, in the weak coupling and Markov approximations. According to Ehrenfest theorem, we require that at short times, $\langle p \rangle$ evolves like in the classical case, which gives $\Gamma = \sqrt{-ln\gamma}$. The first two terms of the Eq. (3) can be reinterpreted as the evolution of an effective non-Hermitian Hamiltonian, $\hat{H}_{eff} = \hat{H}_s + i\hat{W}$, with $\hat{W} = -1/2\sum_\mu \hat{L}_\mu^+ \hat{L}_\mu$. The last term is responsible for the so-called quantum jumps. Given an initial pure state $|\psi(t_0)\rangle$, the jump probabilities dp_μ in an infinitesimal time dt are defined by $dp_\mu = \langle\psi(t_0)|\hat{L}_\mu^+\hat{L}_\mu|\psi(t_0)\rangle dt$, and the new state after the jumps, by $|\psi_\mu\rangle = \hat{L}_\mu|\psi(t_0)\rangle/||\hat{L}_\mu|\psi(t_0)\rangle||$. With probability dp_μ a jump occurs and the system is left in the state $|\psi_\mu\rangle$. With probability $1 - \sum_\mu dp_\mu$ there are no jumps and the system evolves according to the effective Hamiltonian $\hat{H}_{eff}$. The quantum trajectories approach has been used to simulate the master equation Eq. (3) [15]. The numerical evaluation

is made according to the following steps: starting from a pure state $|\psi(t_0)\rangle$, at intervals dt we choose a random number ϵ from a uniform distribution in the unit interval $[0,1]$. If $\epsilon \leq dp$, where $dp = \sum_{\mu=1}^{2} dp_\mu$, the system jumps to one of the states $|\psi_\mu\rangle$ (to $|\psi_1\rangle$ if $0 \leq \epsilon \leq dp_1$ or to $|\psi_2\rangle$ if $dp_1 < \epsilon \leq dp_1 + dp_2$). If $\epsilon > dp$ the evolution with the non-Hermitian Hamiltonian $\hat{H}_s$ takes place ending up in a state that we call $|\psi_0\rangle$. In both circumstances the state is renormalized. Note that we must take dt much smaller than the time scales relevant for the evolution of the open quantum system we are studying. In our simulation, dt is inversely porportional to $\hbar_{eff}$. We can write the mean value $\langle A\rangle_t = Tr[\hat{A}\hat{\rho}(t)]$ as the average over $\mathcal{N}$ trajectories:

$$\langle A\rangle_t = \lim_{\mathcal{N}\to\infty} \frac{1}{\mathcal{N}} \sum_{i=1}^{\mathcal{N}} \langle\psi_i(t)|\hat{A}|\psi_i(t)\rangle \tag{5}$$

It turns out that $\mathcal{N} \approx 100 - 500$ is sufficient to obtain a satisfactory statistical convergence. The simulation of the quantum evolution with quantum trajectories has enormous advantages in memory requirements as it allows us to store only a stochastically evolving state vector instead of a full density matrix.

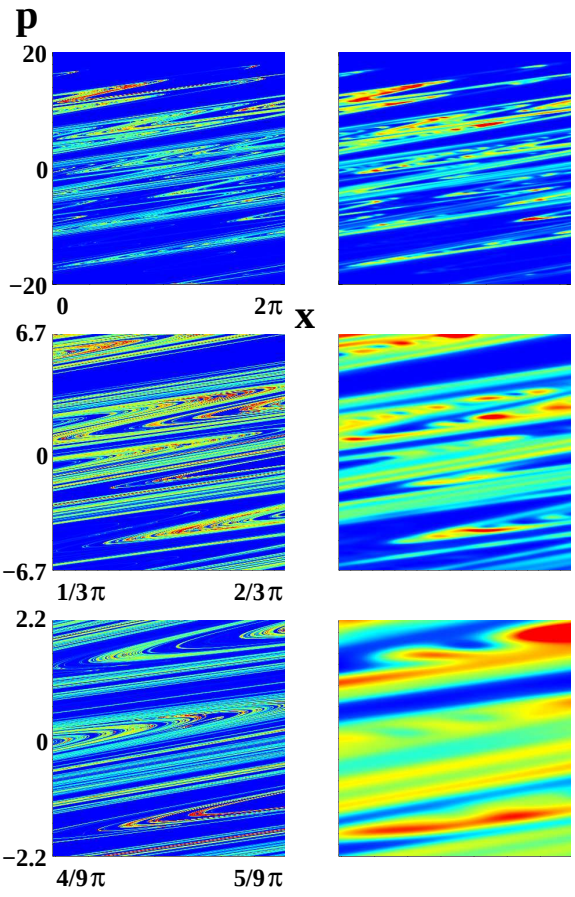

Figure 1. Phase space pictures for $K = 7$, $\gamma = 0.7$, $\phi = \pi/2$ and $a = 0.7$ after 100 kicks: classical Poincaré sections (left) and quantum Husimi funtions at $\hbar_{eff} = 0.012$ (right). In the upper row we display the region $p \in [-20, 20]$ and $x \in [0, 2\pi[$ (note that to draw the attractor, x is taken modulus 2π). Magnifications of these plots are shown in the second and third rows (the area is reduced by a factor 1/9 and 1/81 respectively). The color is proportional to the density: blue for zero and red for maximal density.

In Fig.1 which is drawn for parameter values $K = 7$, $\gamma = 0.7$, $\phi = \pi/2$ and $a = 0.7$, we see the appearance of a strange attractor. In the left panel we show the classical Poincaré section constructed from 10^7 initial conditions uniformly distributed in the area $x \in [0, 2\pi[$, $p \in [-\pi, \pi]$, after 100 iterations of the map Eq. (2). From top to bottom we zoom in, showing the fractal structure of the attractor. On the right panel we show the corresponding Husimi functions of the quantum evolution for $\hbar_{eff} = 0.012$. The Husimi functions are averaged over $N_i = 5$

initial conditions (randomly selected in $p \in [-\pi, \pi]$), considering $\mathcal{N} = 160$ trajectories for each initial condition. Though the quantum version is less detailed, the main classical pattern is well reproduced. In general we can observe a good agreement between the classical and the quantum phase space portraits even though the resolution of the quantum picture is limited by the uncertainty principle. It is also seen that the attractor is strongly asymmetric, suggesting that $\langle p \rangle \neq 0$. This is confirmed in Fig. 2, where $\langle p \rangle$ is shown as a function of time, both in the classical and in the quantum case for different $\hbar_{eff} = 0.037, 0.11, 0.33, 0.99$. A gradual approach to the classical limit can be clearly seen as $\hbar_{eff} \to 0$ in agreement with the correspondence principle.

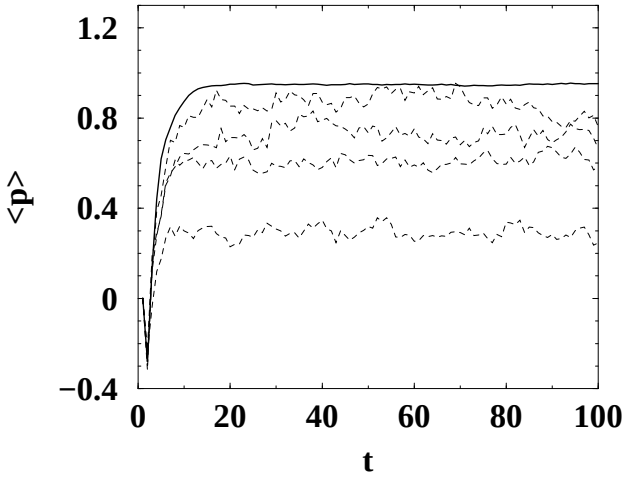

Figure 2. Average momentum $\langle p \rangle$ as a function of time t (measured in number of kicks), with same parameter values as in Fig. 1. The solid curve corresponds to the classical limit while the other curves are quantum results at (from bottom to top) $\hbar_{eff} = 0.99, 0.33, 0.11, 0.037$. Each quantum curve is obtained from $N_i = 60$ initial conditions and $\mathcal{N} = 480$ trajectories for each initial conditions.

It is also possible to control the direction of the transport by varying the phase ϕ. In particular, due to the fact that the potential has the symmetry $V_\phi(x,t) = V_{-\phi}(-x,t)$, it is possible to reverse the current with the transformation $\phi \to -\phi$. We emphasize that our ratchet phenomenon is stable with respect to noise effects and we stress that this robustness is in contrast with the behavior of the quantum Hamiltonian ratchets (see for example [16]). Indeed in our case the ratchet effect is produced by dissipation and therefore it remains stable with the introduction of noise. We also note that the Husimi function can in principle be measured from a state reconstruction technique [17].

3. Chaotic ratchet dynamics with cold atoms in a pair of pulsed optical lattices

In this section we discuss a quantum ratchet which can be realized experimentally by using two consecutive symmetric but dephased kicking potentials instead of only one asymmetric kick (more difficult to realize experimentally). A dissipative process is added [18]. The application of a second kick has some analogy with the model studied in [16]. Dissipation, in this case, is implemented by absorbing boundary conditions. Namely if $\psi(p)$ is the wave-function in the momentum space, we set $\psi(p) = 0$ if $p \leq -p_c$ or $p \geq p_c$. Such boundary condition could be realized experimentally using, for example, velocity selective Raman transitions, which change the internal states of the atoms, and hence let them escape from the state of interest [19]. Moreover, this particle escape mechanism, models the evaporative cooling process typical in cold atom experiments. It is important that the time scale of the absorption mechanism should be of the order of the kicking period to allow for a steady dissipation during the system's evolution. The simplicity of this model is essential for an efficient experimental implementation with cold atoms.

Let us consider a particle moving in one dimension [$x \in (-\infty, +\infty)$] in a periodically kicked potential. The Hamiltonian is:

$$H = \frac{p^2}{2} + V_{\phi,\xi}(x,t), \quad V_{\phi,\xi}(x,t) = k\times \\ \sum_{n=-\infty}^{+\infty}[\delta(t-nT)\cos(x) + \delta(t-nT-\xi)\cos(x-\phi)] \tag{6}$$

where T is the kicking period, k is the kicking strength and ξ ($0 \leq \xi < T$) and ϕ ($0 \leq \phi < 2\pi$) are parameters which change the symmetry characteristics of the system. In this system $\hbar_{eff} = T$. The one-cycle evolution operator is given by:

$$\hat{\mathcal{U}} = e^{-i(T-\xi)\hat{p}^2/2} e^{-ik\cos(\hat{x}-\phi)} e^{-i\xi\hat{p}^2/2} e^{-ik\cos(\hat{x})} \tag{7}$$

The dissipation is realized by projection over a subspace corresponding to the quantum levels that are below p_c (in absolute value). In practice, this dissipation is implemented at each kick. Denoting by $\hat{P}$ the projection operator on the interval $]-p_c, p_c[$, the wave-function after n kicks is given by:

$$\psi(p,n) = \left(\hat{P}\hat{\mathcal{U}}\right)^n \psi(p,0) \tag{8}$$

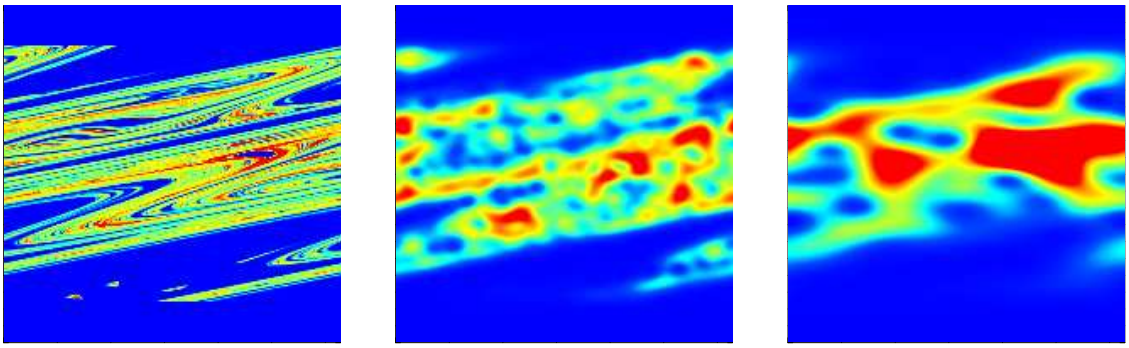

Figure 3. Phase space pictures for $\phi = \pi/2$, at $n = 20$: classical Poincaré sections (left panel), quantum Husimi functions with $\hbar_{eff} \approx 0.16$ (center panel) and $\hbar_{eff} \approx 1$ (right panel). The displayed region is given by $I = pT \in [-20, 20]$ (vertical axis) and $x \in [0.2\pi[$ (horizontal axis). Note that, to draw the repeller, x is taken modulus 2π. The color is proportional to the density: blue for zero and red for maximal density.

In the phase space portraits of Fig. 3 we see the appearance of a strange repeller. These portraits are obtained for $\phi = \pi/2$ and $n = 20$ (after $n = 20$ kicks we are left with approximately 10% of the initial number of particles). The three panels correspond, from left to right, to the classical Poincaré section and the quantum Husimi function at $\hbar_{eff} \approx 0.16$ and $\hbar_{eff} \approx 1$. We have fixed $K = 7$, corresponding to the classical chaotic regime, $\xi = T/3$ and $p_c\hbar_{eff} = 15.2$. The initial state is given by a uniform mixture of momentum states inside the interval $p\hbar_{eff} \in [-1, 1]$. Once the quasi-momentum is fixed (the quasi-momentum is conserved in this system), the number of momentum states in the interval is $\propto 1/\hbar_{eff}$. We also average numerical data over 10^3 randomly chosen quasi-momenta. Classical averages are constructed from 10^7 initial conditions randomly and uniformly distributed in the region $x \in [0, 2\pi[$, $I = pT \in [-1, 1]$. We can see a good agreement between the classical and the quantum phase space portraits. Quantum fluctuations smooth the fractal structure of the classical repeller on the scale of Planck's cell [11]. The repeller is strongly asymmetric suggesting directed transport.

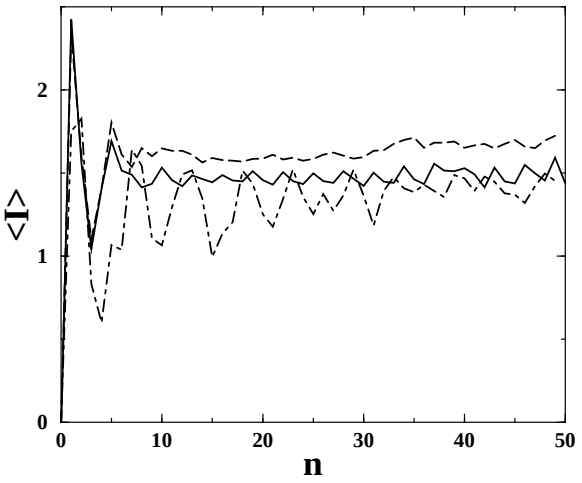

Figure 4. Average rescaled momentum $\langle I\rangle = \langle p\rangle T$ as a function of discrete time n, for the same parameter values as in Fig.3. The solid curve corresponds to quantum results for $\hbar_{eff} \approx 0.16$ and the dotted one to $\hbar_{eff} \approx 1$.

This is confirmed by Fig. 4, where $\langle I\rangle = \langle p\rangle T$ is shown as a function of time n. As discussed in [18] it is possible to explain the origin of the directed current present in our system by following the approach developed in [8].

4. Many-body quantum ratchet in a Bose-Einstein condensate

The realization of Bose-Einstein condensates (BECs) of dilute gases has opened new opportunities for the study of dynamical systems in the presence of many-body interactions. Indeed it is possible to prepare initial states with high precision and to tune over a wide range the many-body, atom-atom interaction. From the viewpoint of directed transport, the study of many-body quantum system is, to our knowledge, at the very beginning.

In this section we consider N condensed atoms confined in a toroidal trap of radius R and cross section πr^2, with the condition $r \ll R$, so that the motion is essentially one-dimensional. The dynamics of a dilute condensate in a pair of periodically kicked optical lattices at zero temperature is described by the Gross-Pitaevskii nonlinear equation,

$$i\frac{\partial}{\partial t}\psi(\theta,t) = \left[-\frac{1}{2}\frac{\partial^2}{\partial\theta^2} + g|\psi(\theta,t)|^2 + V_{\phi,\xi}(\theta,t)\right]\psi(\theta,t), \tag{9}$$

where θ is the azimuthal angle, $g = 8NaR/r^2$ is the scaled strength of the nonlinear interaction (we consider the repulsive case, *i.e.*, $g > 0$), a is the s-wave scattering length for elastic atom-atom collisions. The kicked potential $V_{\phi,\xi}(\theta,t)$ is defined as

$$\begin{gathered} V_{\phi,\xi}(\theta,t) = \textstyle\sum_n [V_1(\theta)\delta(t-nT) + V_2(\theta,\phi)\delta(t-nT-\xi)], \\ V_1(\theta) = k\cos\theta, \;\; V_2(\theta,\phi) = k\cos(\theta-\phi), \end{gathered} \tag{10}$$

where k is the kicking strength and T the period of the kicks. The parameters $\phi \in [0, 2\pi[$ and $\xi \in [0, T[$ are used to break the space and time symmetries, respectively. Note that we set $\hbar = 1$ and that the length and the energy are measured in units of R and $\hbar^2/mR^2$, with m the atomic mass. The wave function normalization reads $\int_0^{2\pi} d\theta |\psi(\theta,t)|^2 = 1$ and we assume periodic boundary conditions, $\psi(\theta + 2\pi, t) = \psi(\theta, t)$.

As shown in the previous section, for the noninteracting case $g = 0$, space-time symmetries are broken when $\phi \neq 0, \pi$ and $\xi \neq 0, T/2$ and therefore there is directed transport in both the classical and quantum case. However, if we take $T = 6\pi$ and $\xi = 4\pi$, then the quantum motion, independently of the kicking strength k, is periodic of period $2T$. In fact,

$$\begin{aligned}
\psi(\theta, 4\pi^+) &= \exp[-iV_1(\theta)]\psi(\theta, 0), \\
\psi(\theta, 6\pi^+) = \exp[-iV_2(\theta,\phi)]\psi(\theta+\pi, 4\pi^+) &= \exp\{-i[V_2(\theta,\phi) - V_1(\theta)]\}\psi(\theta+\pi, 0), \\
\psi(\theta, 10\pi^+) = \exp[-iV_1(\theta)]\psi(\theta, 6\pi^+) &= \exp(-iV_2(\theta,\phi))\psi(\theta+\pi, 0), \\
\psi(\theta, 12\pi^+) &= \exp[-iV_2(\theta,\phi)]\psi(\theta+\pi, 10\pi^+) = \psi(\theta, 0),
\end{aligned} \tag{11}$$

where $\psi(\theta, t^+)$ denotes the value of the wave function at time t just after the kick. The momentum $\langle p(t)\rangle = -i\int_0^{2\pi} d\theta\psi^\star(\theta,t)\frac{\partial}{\partial\theta}\psi(\theta,t)$ also changes periodically with period 12π (4 kicks). Therefore, the average momentum $p_{\rm av} = \lim_{t\to\infty}\overline{p}(t)$ ($\overline{p}(t) = \frac{1}{t}\int_0^t dt'\langle p(t')\rangle$) is given by

$$\begin{aligned}
p_{\rm av} &= \tfrac{4\pi\langle p(0)\rangle + 2\pi\langle p(4\pi^+)\rangle + 4\pi\langle p(6\pi^+)\rangle + 2\pi\langle p(10\pi^+)\rangle}{12\pi} \\
&= \langle p(0)\rangle + \tfrac{k}{2}\int_0^{2\pi}(\sin(\theta) - \sin(\theta-\phi))\,|\psi(\theta,0)|^2 d\theta.
\end{aligned} \tag{12}$$

It is now important to remark that, for the constant initial condition $\psi(t,0) = 1/\sqrt{2\pi}$, which has the important physical meaning of being the ground state of a particle in the trap (hence the initial condition for a Bose-Einstein condensate), the momentum is zero at any time.

It is therefore interesting to study the case of a BEC, because atom-atom interactions may break the above periodicity, and this may cause generation of momentum. Numerical integration of Eq. (9) shows that this is indeed the case. In Fig. 5 it is seen that at $g \neq 0$ the momentum oscillates around a mean value clearly different from zero. Notice that without interactions ($g = 0$) the momentum is exactly zero, so that we have directed transport as a clear signature of the many-body atom-atom interactions.

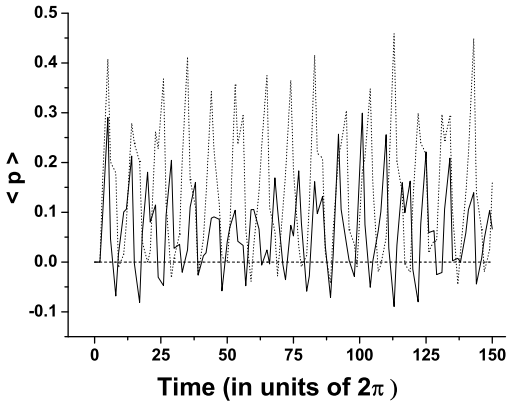

Figure 5. Momentum versus time for different values of interaction strength g, at $k \approx 0.74$ and $\phi = -\pi/4$: $g = 0$ (dashed line), $g = 0.5$ (continuous curve), $g = 1$ (dotted curve).

In actual experiments involving BEC, it is not possible to maintain the coherence of the BEC itself for very long times, especially if the BEC is under a kicking potential. It is therefore reasonable to investigate the value of the momentum after a small number of kicks, let us say 30 kicks and compare it with the asymptotic value. In Fig. 6, we compare the asymptotic value $p_{\rm av}$, obtained from long numerical integrations of the Gross-Pitaevskii equation (dotted line with triangles), with the average of $\langle p(t)\rangle$ over the first 30 kicks ($\bar{p}(90\pi)$(continuous line with boxes). It can be seen that this short-time average is sufficient to obtain a good estimate

of the asymptotic average momentum p_{av}, provided that $g > 0.5$. It is important to remark that the average momentum after the first kicks grows monotonously with g. Therefore, the ratchet current provides a method to measure the interaction strength in an experiment. The inset of Fig. 6 shows how fast the cumulative average $\overline{p}(t)$ converges to the asymptotic limit. As we can already see from the main part of Fig. 6, for strong enough interactions ($g > 0.5$), the convergence to the limiting value $p_{\rm av}$ is rather fast.

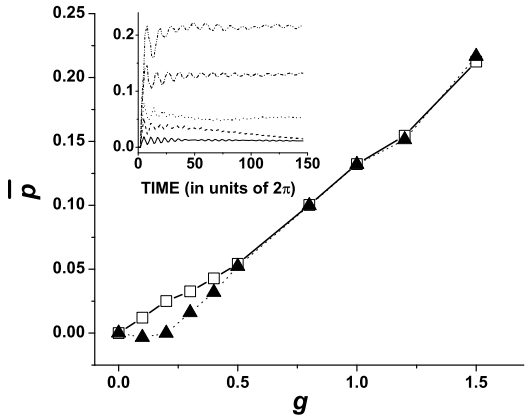

Figure 6. Momentum averaged over the first 30 kicks (solid line with boxes) and asymptotic momentum (dotted line with triangles). Inset: Cumulative average $\overline{p}(t)$ as a function of time for different values of g. From bottom to top $g = 0.1, 0.2, 0.4, 1.0, 1.5$. Parameter values: $k \approx 0.74$, $\phi = -\pi/4$.

It is possible to gain an intuitive understanding on how the interaction induces the generation of a nonzero current. To this end we approximate, for small values of g, the free evolution of the BEC by a split-operator method as in [22]:

$$\psi(\theta,\tau) \approx e^{-i\frac{1}{2}\frac{\partial^2}{\partial\theta^2}\frac{\tau}{2}} e^{-ig|\psi(\theta,\frac{\tau}{2})|^2\tau} e^{-i\frac{1}{2}\frac{\partial^2}{\partial\theta^2}\frac{\tau}{2}} \psi(\theta,0). \tag{13}$$

Using this approximation, we can compute the evolution of the condensate, by taking $\psi(\theta,0) = 1/\sqrt{2\pi}$ as initial condition. To first order in g we obtain $|\psi(\theta,6\pi)|^2 \approx \frac{1}{2\pi}\{1 + g\sin[4V_1(\theta)]\}$. This clarifies the mechanism of the ratchet effect; due to atom-atom interactions, the modulus square of the wave function at time 6π (before the second kick) is no longer constant in θ as it is always the case for a non-interacting BEC. In particular, $|\psi(\theta,6\pi)|^2$ has a different symmetry compared to the second kick. Hence, the current after the kick at time $t = 6\pi^+$ is given by

$$\begin{array}{c} \langle p(6\pi^+)\rangle = -\int_0^{2\pi} d\theta V_2'(\theta,\phi)|\psi(\theta,6\pi)|^2 \\ \approx gk\int_0^{2\pi} d\theta \sin(\theta-\phi)\sin(4k\cos\theta) = -gk\sin(\phi)J_1(4k), \end{array} \tag{14}$$

where J_1 is the Bessel function of the first kind of index 1. This current is, in general, different from zero, provided that $V_2(\theta,\phi)$ is not itself symmetric under $\theta \to -\theta$, that is, when $\phi \neq 0, \pi$.

It is also possible to control the direction of the transport by varying the phase ϕ: the current can be reversed simply by changing $\phi \to -\phi$ as clearly shown in Fig. 7. This current inversion is due to the symmetry of the kicking potential $V(-\theta,\phi,t) = V(\theta,-\phi,t)$.

When studying the dynamics of a kicked BEC, it is important to take into account the proliferation of noncondensed atoms. Strong kicks may lead to thermal excitations out of equilibrium and destroy the condensate. Actually, even before complete destruction of the BEC, a too large number of noncondensed atoms would already render the description by the Gross-Pitaevskii equation meaningless [23, 24].

In [22] we have computed the mean number of noncondensed particles at zero temperature $\delta N(t)$ using the approach developed in [25] (see also [24]). $\delta N(t)$ grows either polynomially

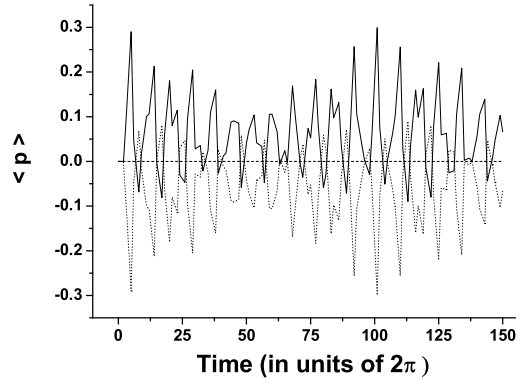

Figure 7. Momentum versus time for different values of the parameter ϕ, at $k \approx 0.74$ and $g = 0.5$: $\phi = -\pi/4$ (continuous curve), $\phi = 0$ (dashed line), $\phi = \pi/4$ (dotted curve).

or exponentially. In the first case the condensate is considered stable since the number of noncondensed particles is negligible up to long times. On the contrary, when the number of noncondensed particles grows exponentially (which is for $g > g_c \approx 1.7$), $\delta N \sim \exp(rt)$, leading to a significant depletion of the condensate after a time $t_d \sim \ln(N)/r$. This is clearly shown in Fig. 8. For instance, $\delta N \approx 0.2$ (10) after $t = 90\pi$ (30 kicks) at $g = 0.5$ (1.5), which is much smaller than the total number of particles $N \approx 10^3 - 10^5$ [24, 28]. This shows that, for the parameter values considered in this paper, the number of noncondensed particles is negligible compared to the number of condensed ones, thus demonstrating that our theoretical and numerical results based on the Gross-Pitaevskii equation are reliable.

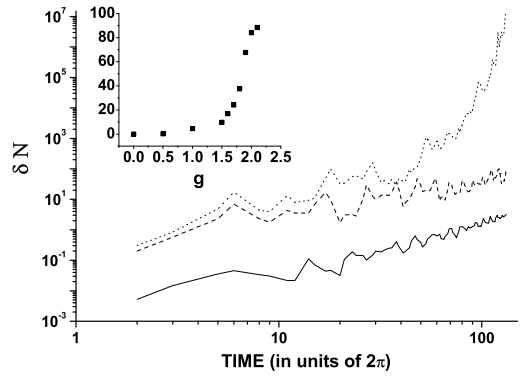

Figure 8. Mean number δN of noncondensed particles versus time for different values of the interaction strength g: from bottom to top, $g = 0.5$, 1.5, and 2.0. Inset: δN vs. g after 30 kicks. Parameter values: $k \approx 0.74$, $\phi = -\pi/4$.

Finally we would like to discuss the experimental feasibility of our proposal. The torus-like potential confining the BEC may be realized by means of optical billiards [26]. The kicks may be applied using a periodically pulsed, strongly detuned laser beam with a suitably engineered intensity, as proposed in [27]. The feasibility is also supported by the latest progresses in the realization of BECs in optical traps such as the ^{87}Rb BEC in a quasi-one-dimensional optical box trap, with condensate length ~ 80 μm, transverse confinement ~ 5 μm, and number of particles $N \sim 10^3$ [28]. In ref.[29], sequences of up to 25 kicks have been applied to a BEC of ^{87}Rb atoms confined in a static harmonic magnetic trap, with kicking strength $k \sim 1$ and in the quantum antiresonance case ($T = 2\pi$) for the kicked oscillator model. Finally, it is possible to tune the interaction strength g over a very large range using a Feshbach resonance [30].

5. Conclusions

The work described in this paper has been inspired by the recent advances in the experimental realization of optical lattices. Cold atoms and Bose-Einstein condensates exposed to time-dependent standing waves of light provide an ideal test bed to explore complex quantum dynamics. We have discussed here two different models of dissipative quantum ratchets: in the first one the quantum noise is modeled via the quantum trajectories method, while in the second one the dissipation is described by evaporative cooling. Due to the presence of quantum strange attractors the stationary current is independent of initial conditions. State reconstruction techniques could in principle allow experimental observation of a quantum strange ratchet set. We have also discussed a model of a conservative quantum ratchet where transport is generated by the atom-atom interaction in the BEC.

References

[1] Moore F L, Robinson J C, Bharucha C F, Sundaram B and Raizen M G 1995 *Phys. Rev. Lett.* **75** 4598
Ringot J, Szriftgiser P and Garreau J C 2000 *Phys. Rev. Lett.* **85** 2741
[2] Ammann H, Gray R, Shvarchuck I and Christensen N 1998 *Phys. Rev. Lett.* **80** 4111
[3] d'Arcy M B, Godun R M, Oberthaler M K, Cassettari D and Summy G S 2001 *Phys. Rev. Lett.* **87** 074102
[4] Steck D A, Oskay W M and Raizen M G 2001 *Science* **293** 274
Hensinger W K, Haffner H, Browayes A, Heckenberg N R , Helmerson K, McKenzie C, Milburn G J, Phillips W D, Rolston S L, Rubinsztein-Dunlop H and Upcroft B 2001 *Nature* **412** 52
[5] Casati G and Chirikov B 1995 *Quantum Chaos: Between Order and Disorder* (Cambridge: Cambridge Univ. Press)
Izrailev F M 1990 *Phys. Rep.* **196** 299
[6] Mennerat-Robilliard C, Lucas D, Guibal S, Tabosa J, Jurczak C, Courtois J Y, and Grynberg G 1999 *Phys. Rev. Lett.* **82** 851
Schiavoni M, Sanchez-Palencia L, Renzoni F and Grynberg G 2003 *Phys. Rev. Lett.* **90** 094101
[7] Astumian R D and Hanggi P 2002 *Physics Today* **55** (11) 33
Reimann P 2002 *Phys. Rep.* **361** 57
[8] Flach S, Yevtushenko O and Zolotaryuk Y 2000 *Phys. Rev. Lett.* **84** 2358
[9] Julicher F, Ajdari A and Prost J 1997 *Rev. Mod. Phys.* **69** 1269
[10] Ott E 1993 *Chaos in dynamical systems* (Cambridge: Cambridge Univ. Press)
[11] Dittrich T and Graham R 1990 *Annals of Physics* **200** 363
[12] Carlo G G, Benenti G, Casati G and Shepelyansky D 2005 *Phys. Rev. Lett.* **94** 164101
[13] Sagdeev R Z, Usikov D A and Zaslavskii G M 1988 *Nonlinear Physics: From the Pendulum to Turbulence and Chaos* (New York: Harwood Acad. Publ.)
[14] Lindblad G 1976 *Commun. Math. Phys.* **48** 119
Gorini V and Kossakowski A 1976 *J. Math. Phys.* **17** 821
[15] Dalibart J and Castin Y 1992 *Phys. Rev. Lett.* **68** 580
[16] Jones P H, Stocklin M M, Hur G and Monteiro T S 2004 *Phys. Rev. Lett.* **93** 223002
Hur G, Creffield C E, Jones P H and Monteiro T S 2005 *Phys. Rev.* A **72** 013403
H Lignier, Chabe J, Delande D, Garreau J C and Szriftgiser P 2005 *Phys. Rev. Lett.* **95** 234101
[17] Bienert M, Haug F, Schleich W P and Raizen M G 2002 *Phys, Rev. Lett.* **89** 050403
[18] Carlo G G, Benenti G, Casati G, Wimberger S, Morsch O, Mannella R and Arimondo E 2006 *Phys Rev.* A **74** 033617
[19] Kasevich M, Weiss D S, Riis E, Moler K, Kasapi S and Chu S 1991 *Phys. Rev. Lett.* **66** 2297
[20] Poletti D, Benenti G, Casati G and Li B 2006 Many-body quantum ratchet in a Bose-Einstein condensate *Preprint* cond-mat/0609535
[21] Gommers R, Denison S and Renzoni F 2006 *Phys. Rev. Lett.* **96** 240604
[22] Poletti D, Fu L, Liu J and Li B 2006 *Phys. Rev.* E **73** 056203
[23] Gardiner S A, Jaksch D, Dum R, Cirac J I and Zoller P 2000 *Phys. Rev.* A **62** 023612
[24] Zhang C, Liu J, Raizen M G and Niu Q 2004 *Phys. Rev. Lett.* **92** 054101
Liu J, Zhang C, Raizen M G and Niu Q 2006 *Phys. Rev.* A **73** 013601
[25] Castin Y and Dum R 1997 *Phys. Rev. Lett.* **79** 3553
Castin Y and Dum R 1998 *Phys. Rev.* A **57** 3008
[26] Milner V, Hanssen J L, Campbell W C and Raizen M G 2001 *Phys. Rev. Lett.* **86** 1514
Friedman N, Kaplan A, Carasso D and Davidson N 2001 *Phys. Rev. Lett.* **86** 1518
[27] Mieck B and Graham R 2004 *J. Phys.* A **37** L581

[28] Meyrath T P, Schreck F, Hanssen J L, Chuu C S and Raizen M G 2005 *Phys. Rev.* A **71** 041604(R)
[29] Duffy G J, Mellish A S, Challis K J and Wilson A C 2004 *Phys. Rev.* A **70** 041602(R)
[30] Donley E A, Claussen N R, Cornish S L, Roberts J L, Cornell E A and Wieman C E 2001 *Nature* (London) **412** 295